

Supporting Information

Violet Phosphorus: An Effective Metal-Free Elemental Photocatalyst for Hydrogen Evolution

Mengyue Gu,^a Lihui Zhang,^a Siman Mao,^a Yajun Zou,^a Dandan Ma,^a Jianwen Shi,^a Na Yang,^a Chengcheng Fu,^a Xuewen Zhao,^a Xuequan Xu,^a Yonghong Cheng,^a and Jinying Zhang,^{*a}

^a State Key Laboratory of Electrical Insulation and Power Equipment, Center of Nanomaterials for Renewable Energy, School of Electrical Engineering, Xi'an Jiaotong University, Xi'an 710049, China.

E-mail: jinying.zhang@mail.xjtu.edu.cn

Experimental Section

Synthesis of Violet Phosphorus. 470 mg of amorphous red phosphorus (Aladdin, 99.999% metals basis), 10 mg of Sn (Alfa Aesar, 99.995% metals basis) and 18 mg of SnI₄ (Alfa Aesar, 99.998% metals basis) were put into a quartz glass tube with 14 cm long and 10 mm in diameter. Then the quartz glass tube was evacuated and sealed. Finally, it was placed horizontally into the three-zone muffle furnace. The side of quartz glass tube with source and the other empty side were heated to 650 °C and 630 °C in 8 h, respectively, which were kept at these temperatures for 5 h. Then the quartz glass tube was cooled at 10 °C·h⁻¹ to 550 °C at one side of the source and 530 °C at the other side. Both sides were maintained at this temperature for 30 h. The sample was finally slowly cooled to room temperature for 70 h. Violet phosphorus was obtained.

Preparation of Violet Phosphorus Suspension. Violet phosphorus was ground with an agate mortar and pestle. About 10 mg ground violet phosphorus was added to 20 mL deionized water. The whole system was subjected to ultrasonic treatment for 40min with 30 % amplitude and 1 h 25 min with 20 % amplitude (5 s on and 5 s off) using an ice bath.

Characterization. Transmission electron microscopy (TEM) images and high-resolution TEM (HRTEM) images were acquired by Lorenz Transmission Electron Microscope (Talos F200X). Scanning electron microscopy (SEM) images were recorded by Quanta 250FEG equipment. Atomic force microscope (AFM) images were acquired by Bruker Dimension ICON. X-ray diffraction patterns were obtained from a Bruker D2 PHASER using Cu/K α radiation ($\lambda = 1.5418\text{\AA}$) at 40 kV and 30 mA. Raman spectroscopy was taken in a back-scattering geometry using a single monochromator with a microscope (Reinishaw in Via) equipped with CCD array detector and an edge filter. The samples were excited by laser with wavelength of 633 nm. FT-IR spectra were recorded on a Micro-Infrared Spectroscopy (Bruker VERTEX70). The scanning wavelength range was 400-4000 cm⁻¹. UV-vis-NIR spectrometer (JASCO, V-670) was used to measure the optical features. The fluorescence spectra were achieved using an

Edinburgh FLS980 instrument. X-ray photoelectron spectroscopy (XPS) spectra were obtained using a Thermo Fisher ESCALAB spectrometer.

Photocatalytic Measurements. The photocatalytic H₂ evolution reactions were carried out under UV-vis light irradiation (350 nm - 780 nm) in a quartz cell connected to a glass closed gas circulation and evacuation system (CEL-SPH2N, CEAULIGHT, Beijing). A 300 W Xe-lamp was used as light source (CEL-PF300-T8). The production of H₂ was detected by an online gas chromatography with TCD detector (GC-9720). High pure nitrogen gas was used as carrier gas. In a photocatalytic reaction, 20 mL suspension of violet phosphorus (10 mg violet phosphorus and 20 mL deionized water) was mixed with various sacrificial reagents, including methanol (MeOH, 5 mL), triethanolamine (TEOA, 5mL), lactic acid (HL, 5mL) and Na₂S+Na₂SO₃ (0.75 M+1.05 M) and Pt (0.5 wt.%, 1.0 wt.%, 1.5 wt.%, 2.0 wt.%) as a co-catalyst. The system was vacuumed to remove air before the suspension was irradiated.

Deduction of Band Gaps. The valence band potentials of the corresponding vacuum ($E_{VB, VAC}$) were calculated for violet phosphorus and black phosphorus, respectively, according to equations (S1) and (S2)^{1, 2}:

$$E_{VB, NHE} = \phi + E_{VB, XPS} - 4.44 \quad (S1)$$

where $E_{VB, NHE}$ is the valence band potentials of the corresponding standard hydrogen electrode. ϕ is the work function of the instrument (4.69 eV).

$$E_{VB, VAC} = -4.5 - E_{VB, NHE} \quad (S2)$$

Deduction of Apparent Quantum Efficiency (AQE). 50 mg of violet phosphorus powder was dispersed in 100 mL aqueous solution containing 20 mL MeOH and 1.0 wt.% Pt, which was irradiated for 3 h by a 300 W Xe-lamp using a 365 or 420 nm bandpass filter. The AQE was calculated according to equations (S3) and (S4).³

$$N = \frac{P_{ph} \times t \times \lambda}{hc} \quad (S3)$$

where P_{ph} is the power of the incident light, t is the irradiation time, λ is the wavelength of the incident light, h is planck constant, c is the speed of light in vacuum.

$$\begin{aligned} AQE &= \frac{\text{the number of reacted electrons}}{\text{the number of incident photons}} \times 100\% \\ &= \frac{2 \times \text{the number of evolved } H_2 \text{ molecules}}{N} \times 100\% \end{aligned} \quad (S4)$$

Photoelectrochemical Measurements. The photocurrent response and electrochemical impedance spectroscopy (EIS) were measured on CHI760E electrochemical workstation equipped with a three-electrode system with a working electrode, a platinum sheet as counter electrode and an Ag/AgCl reference electrode. The working electrode was prepared by drop coating, where the sample (1 mg) was dispersed in a mixture (100 μ L) of deionized water and ethanol (2:1) on FTO glass by ultrasonic treatment, and then dried. The Na₂SO₄ aqueous solution (0.5 M) was used as electrolyte and a 300 W Xe-lamp (CEL-PF300-T8) was used as light source.

Detection of photogenerated OH radicals. 30 mg of violet phosphorus powder was dispersed in 40 mL of the stock terephthalic acid solution with final concentrations of 4×10^{-4} M terephthalic acid and 2×10^{-3} M NaOH. The solution was stirred and irradiated. At every 30 min, 1.5 mL of the suspensions were collected and centrifugated. The resulted supernatants were diluted four times for PL measurements. Fluorescence spectra of generated 2-hydroxyterephthalic acid were measured on an Edinburgh FLS980 fluorescence spectrophotometer with an excitation wavelength of 320 nm.^{4,5}

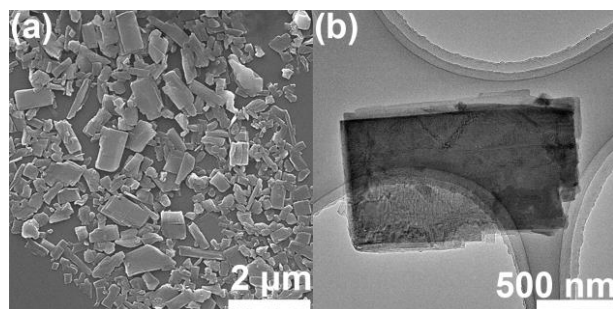


Fig. S1 (a) SEM and (b) TEM images of the as-dispersed violet phosphorus.

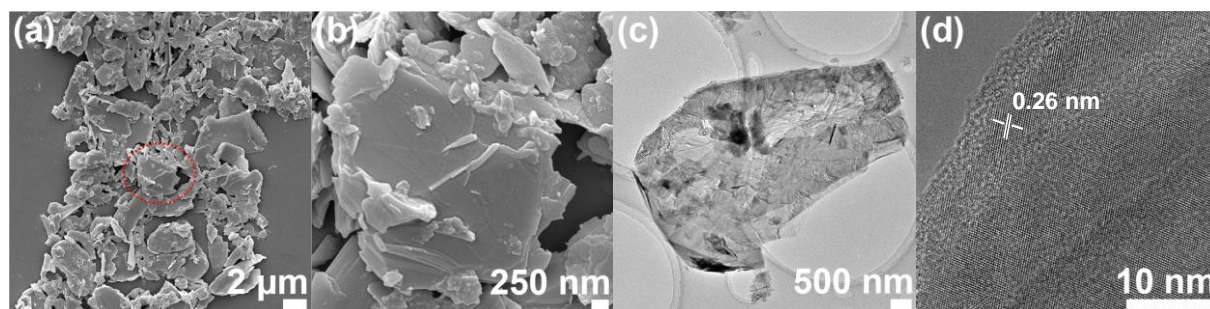


Fig. S2 SEM images of (a) the as-dispersed black phosphorus and (b) magnified image (the red circle), (c) TEM and (d) HRTRM images of the as-dispersed black phosphorus.

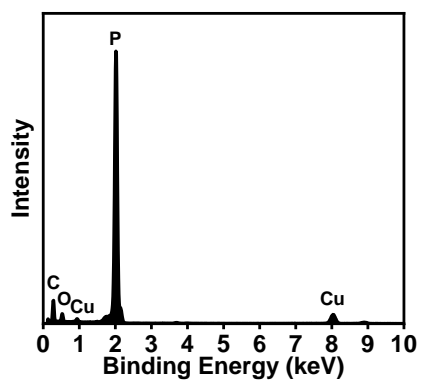


Fig. S3 EDS spectrum of the as-dispersed violet phosphorus.

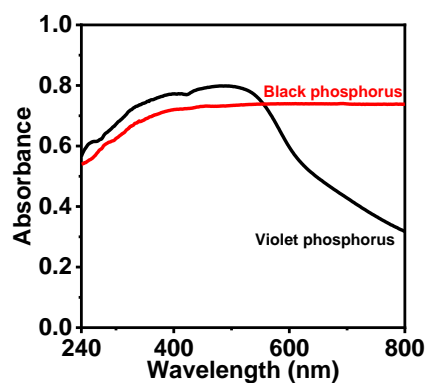


Fig. S4 Absorption spectrum of as-dispersed violet phosphorus compared to that of as-dispersed black phosphorus.

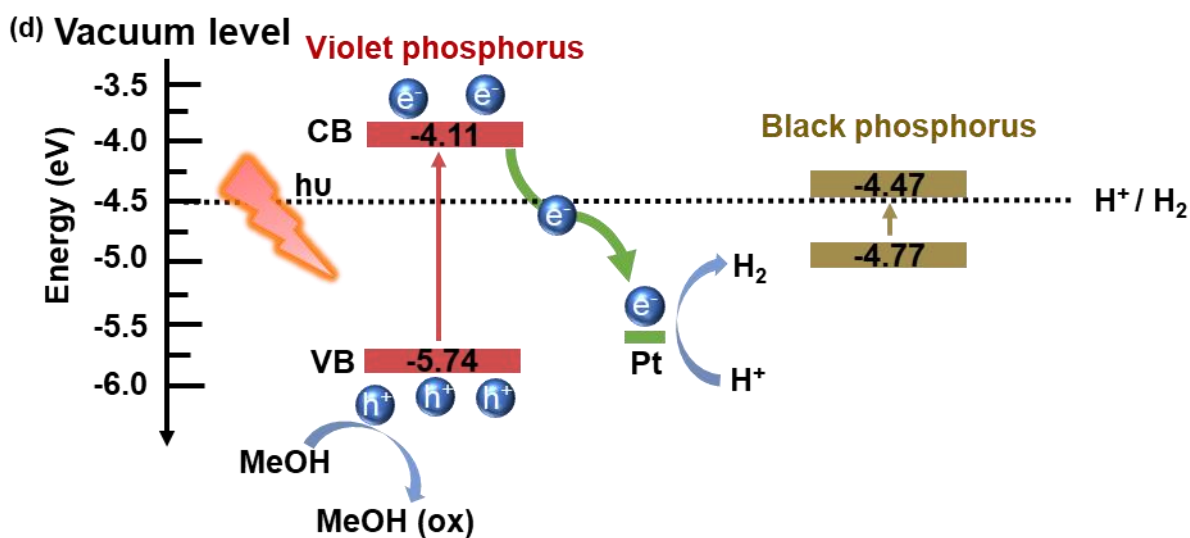
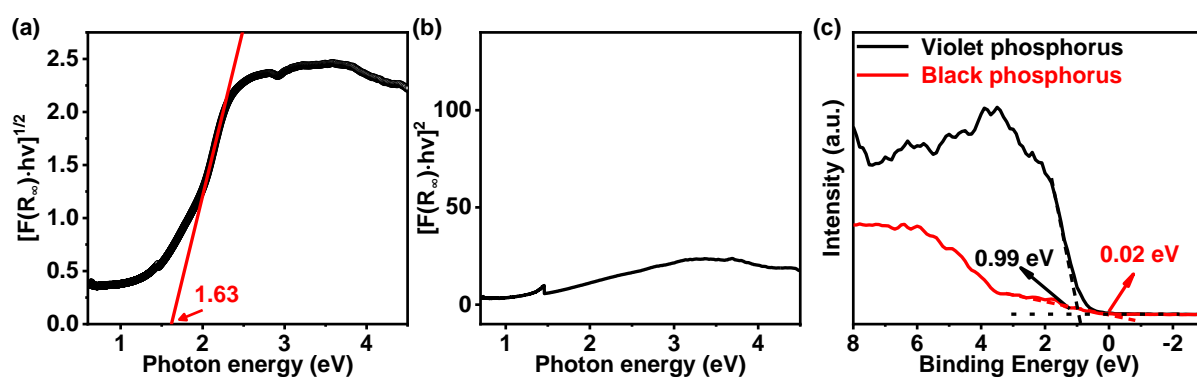


Fig. S5 Diffuse reflectance spectra of (a) violet phosphorus and (b) black phosphorus based on Kubelka-Munk function. (c) Valence band XPS. (d) Schematic diagram of the deduced band edges of violet phosphorus and black phosphorus for photocatalytic reactions.

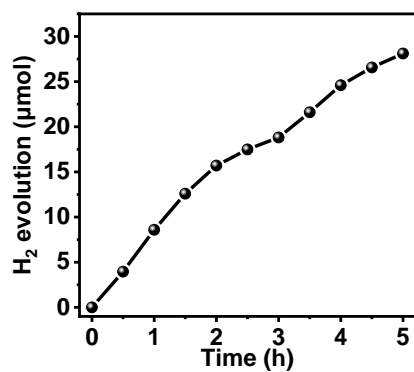


Fig. S6 Time course of photocatalytic H₂ evolution on violet phosphorus.

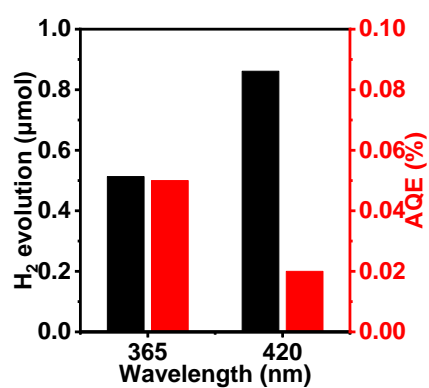


Fig. S7 The H₂ evolution and AQE of violet phosphorus aqueous dispersion containing 20 mL MeOH and 1.0 wt.% Pt irradiated by 365 nm and 420 nm light for 3 h.

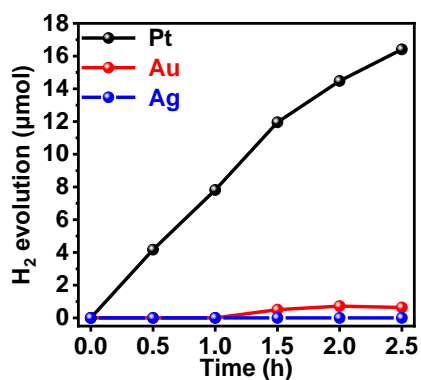


Fig. S8 Time course of H₂ evolution on violet phosphorus with different co-catalysts.

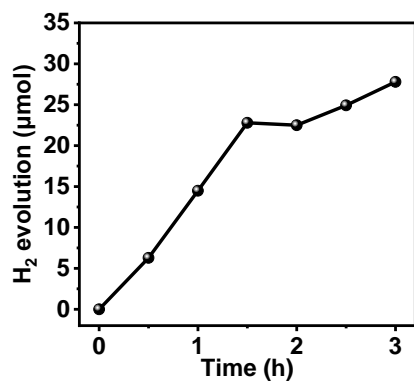


Fig. S9 Time course of H₂ evolution on violet phosphorus with 3.0 wt.% of co-catalyst Pt.

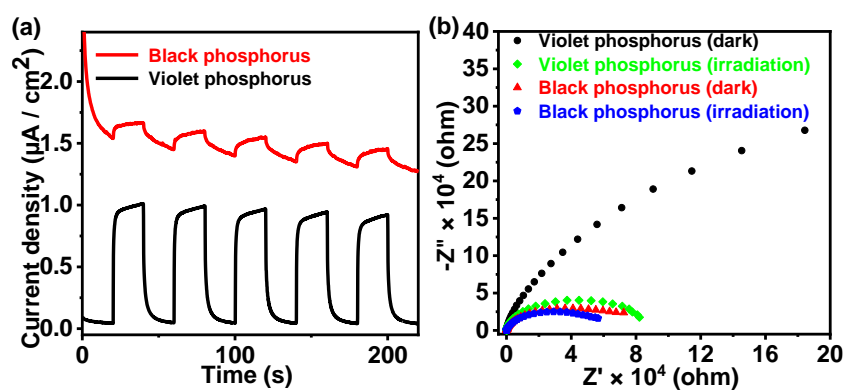


Fig. S10 (a) The photocurrent response and (b) electrochemical impedance spectra (EIS) of violet phosphorus and black phosphorus.

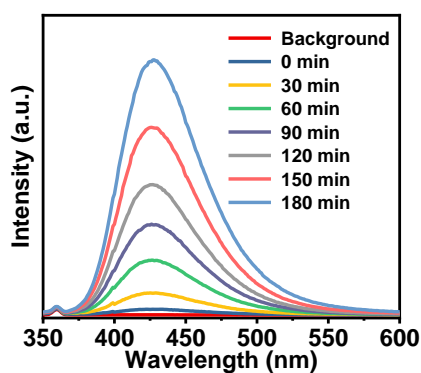


Fig. S11 Time-dependent fluorescence spectra of violet phosphorus.

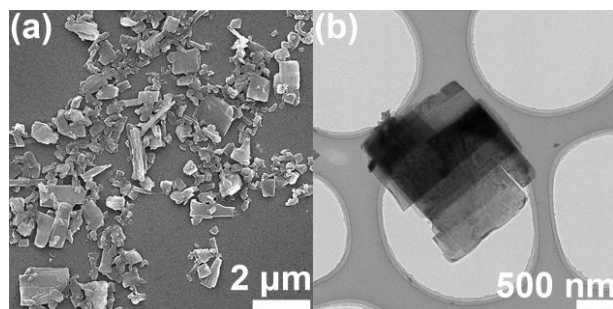


Fig. S12 (a) SEM and (b) TEM images of violet phosphorus after photocatalytic H₂ evolution reaction for 3 h.

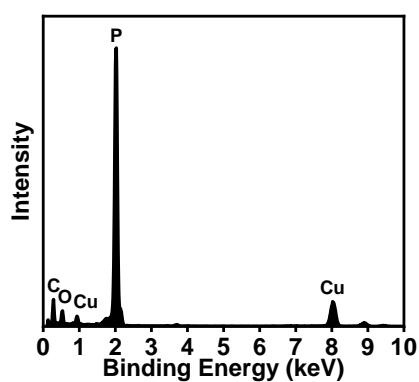


Fig. S13 The EDS spectrum of violet phosphorus after photocatalytic H₂ evolution reaction for 3 h.

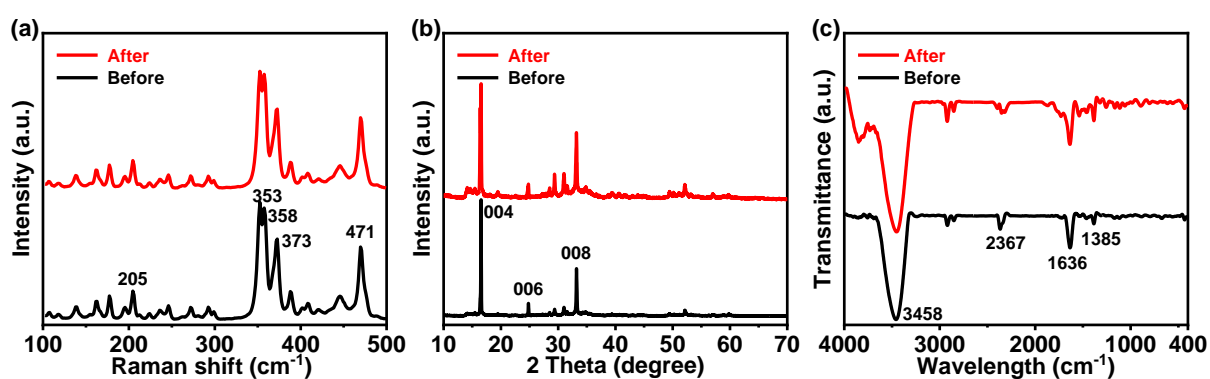


Fig. S14 (a) Raman, (b) XRD and (c) FT-IR spectra of violet phosphorus before (black) and after (red) photocatalytic H₂ evolution reactions.

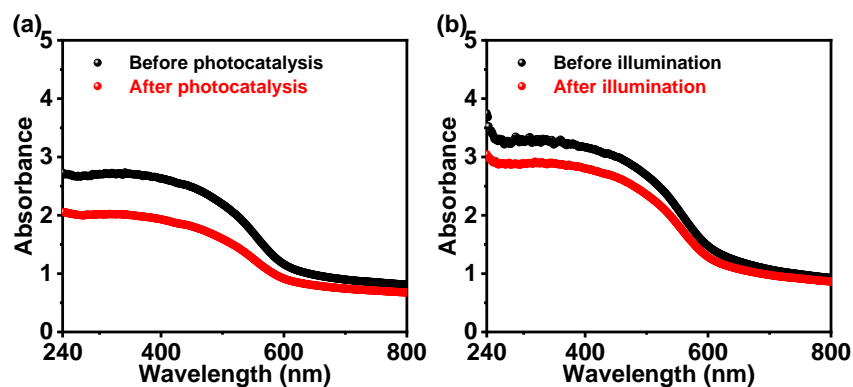


Fig. S15 Absorption spectra of violet phosphorus before and after (a) photocatalytic H_2 evolution reactions and (b) UV-vis (350 - 780 nm) illumination for 3 hours.

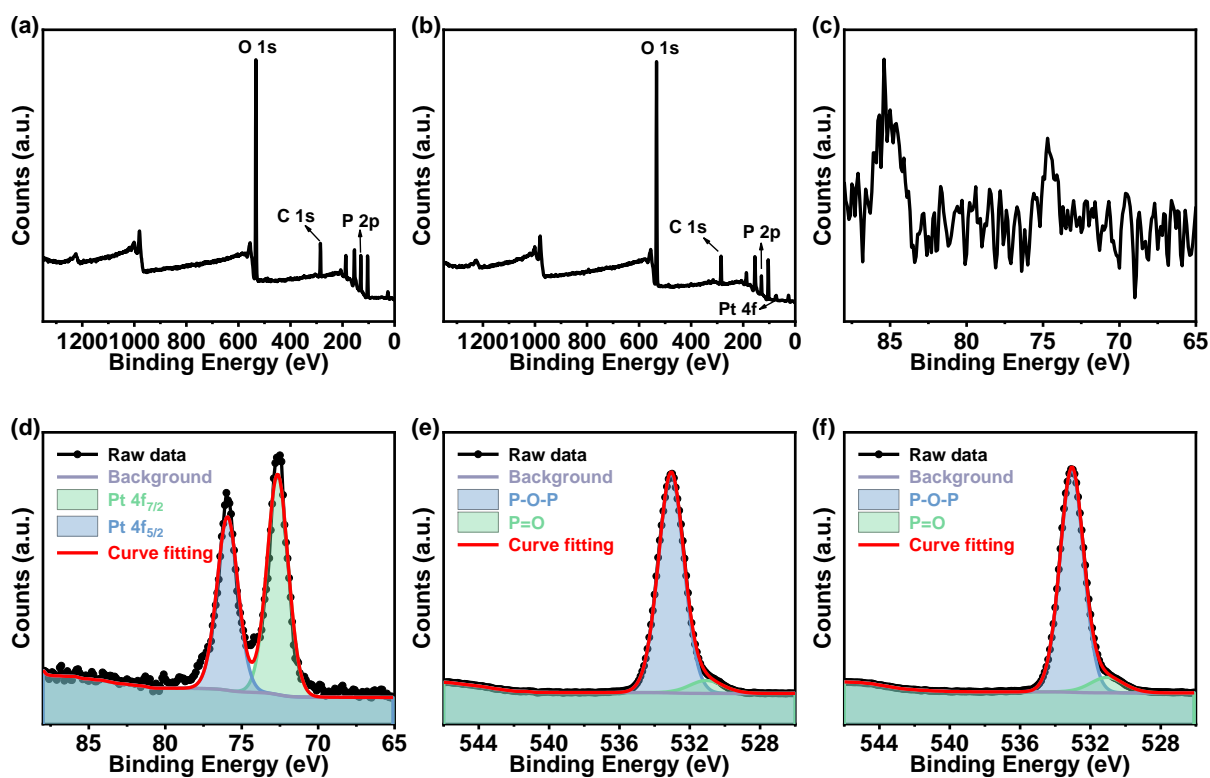


Fig. S16 (a-b) XPS survey spectra, high-resolution XPS spectra of (c-d) O 1s and (e-f) Pt 4f of violet phosphorus before and after photocatalytic H_2 evolution reactions.

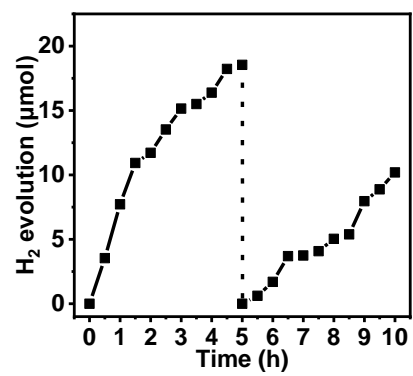


Fig. S17 Cyclic runs of photocatalytic H₂ evolution on violet phosphorus.

Table S1. The photocatalytic activities of black phosphorus and red phosphorus in H₂ evolution.

Photocatalyst	Activity [$\mu\text{molh}^{-1}\text{g}^{-1}$]	Co-catalyst	Sacrificial agent	Light source	Reference
Amorphous RP / Crystalline RP	0.6 / 1.6	-	5 vol.% MeOH	300W Xe lamp ($\lambda > 400 \text{ nm}$)	4
Micro-fibrous P/SiO ₂ / Smashed-fibrous P	633 / 684	Pt	10 vol.% MeOH	300W Xe lamp ($\lambda > 420 \text{ nm}$)	6
Single crystal red P microbelts (PMBs)	513.3	1.0 wt.% Pt	10 vol.% MeOH	300W Xe lamp ($\lambda > 420 \text{ nm}$)	7
Crystalline red phosphorus microbelts (CRPMBs)	553.4	1.0 wt.% Pt	10 vol.% MeOH	300W Xe lamp ($\lambda > 420 \text{ nm}$)	8
Bulk BP / BP-BM	28 / 512	-	0.75 M Na ₂ S and 1.05 M Na ₂ SO ₃	300W Xe lamp ($\lambda > 420 \text{ nm}$)	3
BP nanosheets / BP nanoparticles	64 / 45	-	1.76 mL TEOA	300W Xe lamp ($\lambda > 420 \text{ nm}$)	9
BP nanosheets	447	20.0 wt.% Pt	-	300W Xe lamp ($\lambda > 420 \text{ nm}$)	10
Ethylenediamine- intercalated quasi- monolayer BP (eda- BP)	451.8	3.0 wt.% Pt	0.3 g EDTA	300W Xe lamp ($420 \text{ nm} < \lambda < 780 \text{ nm}$)	11
Bulk BP / BP nanosheets	25.7 / 74.8	-	0.05 M Oxalic acid	300W Xe lamp ($\lambda \geq 420 \text{ nm}$)	12
BP nanoflakes	138	-	Na ₂ S and Na ₂ SO ₃	300W Xe lamp ($\lambda > 420 \text{ nm}$)	13
Violet phosphorus	675 \pm 109	1.0 wt.% Pt	20 vol.% MeOH	300W Xe lamp ($350 \text{ nm} < \lambda < 780 \text{ nm}$)	This work

Table S2. The element contents of violet phosphorus before and after photocatalytic H₂ evolutions from EDS spectra.

Element	Atomic Fraction (%)		Mass Fraction (%)	
	Before	After	Before	After
P	82.9	79.2	92.1	89.9
O	3.8	6.5	2.2	3.8
C	13.3	14.4	5.7	6.3

References

1. X. B. Li, B. B. Kang, F. Dong, Z. Q. Zhang, X. D. Luo, L. Han, J. T. Huang, Z. J. Feng, Z. Chen, J. L. Xu, B. L. Peng and Z. L. Wang, *Nano Energy*, 2021, **81**, 11.
2. M. Gratzel, *Nature*, 2001, **414**, 338-344.
3. X. J. Zhu, T. M. Zhang, Z. J. Sun, H. L. Chen, J. Guan, X. Chen, H. X. Ji, P. W. Du and S. F. Yang, *Adv. Mater.*, 2017, **29**, 7.
4. F. Wang, W. K. H. Ng, J. C. Yu, H. J. Zhu, C. H. Li, L. Zhang, Z. F. Liu and Q. Li, *Appl. Catal. B-Environ.*, 2012, **111**, 409-414.
5. R. Shi, F. L. Liu, Z. Wang, Y. X. Weng and Y. Chen, *Chem. Commun.*, 2019, **55**, 12531-12534.
6. Z. F. Hu, L. Y. Yuan, Z. F. Liu, Z. R. Shen and J. C. Yu, *Angew. Chem.-Int. Edit.*, 2016, **55**, 9580-9585.
7. Y. Liu, Z. F. Hu and J. C. Yu, *Appl. Catal. B-Environ.*, 2019, **247**, 100-106.
8. S. Zhang, S. F. Ma, X. D. Hao, Y. T. Wang, B. Cao, B. Han, H. Zhang, X. G. Kong and B. S. Xu, *Nanoscale*, 2021, **13**, 18955-18960.
9. S. K. Muduli, E. Varrla, Y. Xu, S. A. Kulkarni, A. Katre, S. Chakraborty, S. Chen, T. C. Sum, R. Xu and N. Mathews, *J. Mater. Chem. A*, 2017, **5**, 24874-24879.
10. B. Tian, B. N. Tian, B. Smith, M. C. Scott, Q. Lei, R. N. Hua, Y. Tian and Y. Liu, *Proc. Natl. Acad. Sci. U. S. A.*, 2018, **115**, 4345-4350.
11. Z. J. Sun, H. Miao, M. Khurram, Z. M. Zhang, Y. F. Zhu and Q. F. Yan, *Chem. Eng. J.*, 2021, **421**, 10.
12. S. T. Zhu, Q. S. Liang, Y. T. Xu, H. P. Fu and X. F. Xiao, *Eur. J. Inorg. Chem.*, 2020, **2020**, 773-779.
13. T. M. Zhang, Y. Y. Wan, H. Y. Xie, Y. Mu, P. W. Du, D. Wang, X. J. Wu, H. X. Ji and L. J. Wan, *J. Am. Chem. Soc.*, 2018, **140**, 7561-7567.